Accepted Manuscript

Recycling of end-of-life reverse osmosis membranes for membrane biofilms reactors (MBfRs). Effect of chlorination on the membrane surface and gas permeability.

Jesús Morón-López, Lucía Nieto-Reyes, Sonia Aguado, Rehab El-Shehawy, Serena Molina

PII: S0045-6535(19)31014-8

DOI: https://doi.org/10.1016/j.chemosphere.2019.05.108

Reference: CHEM 23843

To appear in: *ECSN*

Received Date: 21 November 2018

Revised Date: 14 February 2019

Accepted Date: 14 May 2019

Please cite this article as: Morón-López, Jesú., Nieto-Reyes, Lucí., Aguado, S., El-Shehawy, R., Molina, S., Recycling of end-of-life reverse osmosis membranes for membrane biofilms reactors (MBfRs). Effect of chlorination on the membrane surface and gas permeability., *Chemosphere* (2019), doi: https://doi.org/10.1016/j.chemosphere.2019.05.108.

Recycling of End-of-life reverse osmosis membranes for Membrane Biofilms Reactors (MBfRs). Effect of chlorination on the membrane surface and gas permeability.

Jesús Morón-López[1,2*], Lucía Nieto-Reyes[1], Sonia Aguado[2], Rehab El-Shehawy[1,3] and Serena Molina[1]

[1]IMDEA Water Institute, Punto Com. nº 2. 28805, Alcalá de Henares, Madrid, Spain.

[2]Chemical Engineering Department, University of Alcalá, Ctra. Madrid-Barcelona Km 33,600, 28871 Alcalá de Henares, Madrid, Spain.

[3]Department of Environmental Science and Analytical Chemistry, Stockholm University, Sweden.

jesus.moron@imdea.org (J. M-L); lucia.nietoreyes@gmail.com (L. N-R); sonia.aguado@uah.es (S. A); rehab.elshehawy@aces.su.se (R. E-S); serena.molina@imdea.org (S. M).

*Corresponding Author, email: jesus.moron@imdea.org

Keywords: Recycled membranes, transformation process, chlorination, fouling, biofilm, microcystin, degradation, gas permeability.

Graphical Abstract

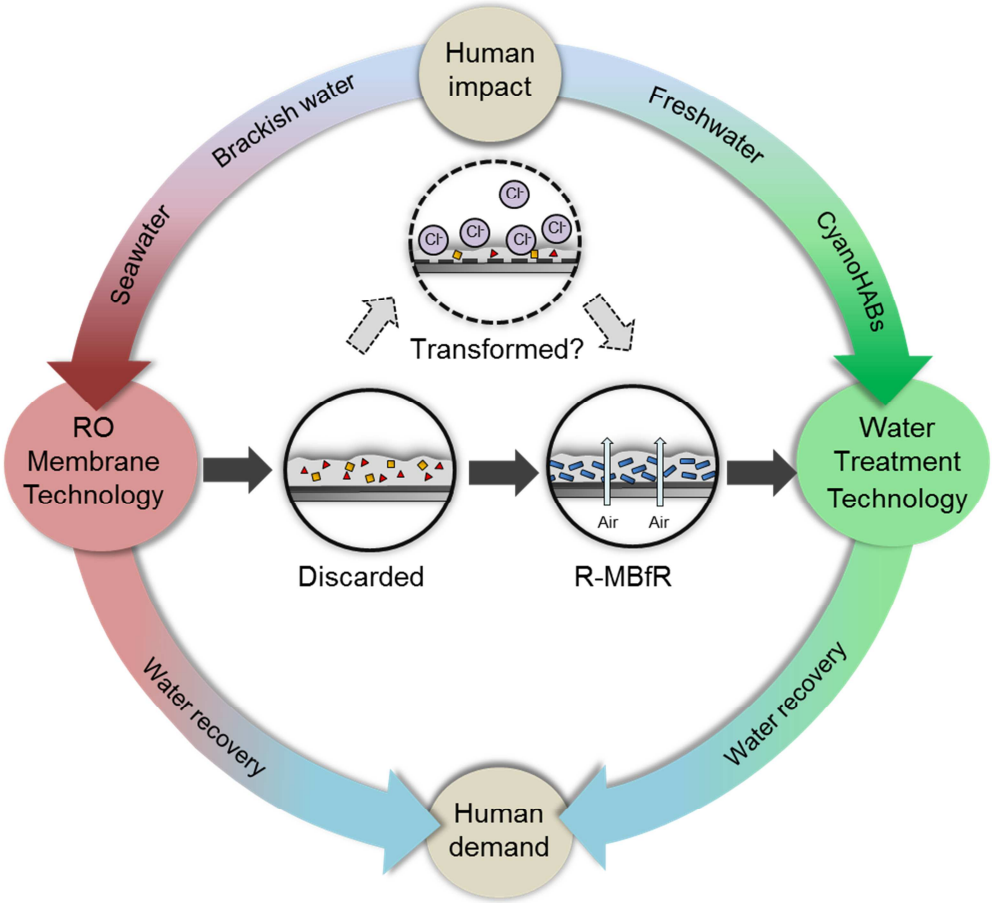

Abstract

Reducing human impacts on drinking water is one of the main challenges for the water treatment industry. This work provides new results to support the recycling of EoL desalination reverse osmosis (RO) membranes for Membranes Biofilm Reactors (MBfRs). We investigate if the controlled-removal of fouling and polyamide layer may favor the use of these membranes in MBfRs. It also would allow establishing a normalized methodology of membrane recycling, regardless of inherited fouling during its lifespan. For this purpose, we transform by chlorination discarded brackish (BWd) and seawater (SWd) membranes into nanofiltration (BWt-NF and SWt-NF) and ultrafiltration (BWt-UF and SWt-UF) membranes. Our results show that chlorine attacks allow the fouling cleaning while improves the hydrophilicity and maintains roughness only in BWt-NF. Therefore, the bacterial deposition in this membrane is greater than the other tested membranes. Besides, the microcystin (MC) degradation capacity of BWt-NF verifies the compatibility of the chemical modification for the biological activity of MC-degrading bacteria. Finally, our results also provide that polyamide thin-film composite (PA-TFC) membranes, originally manufactured for salt rejection during desalination processes, offer competitive gases diffusion at low pressures. Therefore, we conclude that the membrane recycling may provide alternative low cost and gas permeable membranes for MBfRs, according to circular economy principles.

1. Introduction

Water is essential for human life and plays an important role in many sectors of the economy. The strong anthropogenic impact on freshwater worldwide has led to global concern about water supply (Paerl and Paul, 2012; Vörösmarty et al., 2000). The ever-growing human population, and increasing water pollution and freshwater demands, have allowed major advances to be made in water treatment processes (Ercin and Hoekstra, 2014; M.Mekonnen and Hoekstra, 2016). Membrane technology is among the most important fields in the separation processes employed for water treatment. The use of membrane separation technology has several advantages: continuous operation, adjusted properties of membranes to the requirements set in each application, flexibility in systems design and easy scaling-up. Therefore, membrane technology has considerably developed in recent decades to establish a solid, mature and standardized market.

Pressure-driven membranes are well-established desalination processes by which freshwater can be obtained from seawater and brackish water (Van Der Bruggen et al., 2003). In particular, reverse osmosis (RO) membranes constitute the most used desalination technology worldwide. Over 95% of existing RO desalination plants use polyamide thin film composite (PA-TFC) membranes, a high-performance material with excellent mechanical and chemical durability (Geise et al., 2010). Consequently, the large desalination market has resulted in increased waste generation associated with this technology, which has led to the disposal of more than 840,000 end-of-life (EoL) membranes (>14,000 Tn/year) every year worldwide (Landaburu-Aguirre et al., 2016; Peng Lee et al., 2011). The landfilling or incineration of millions of

membranes is currently the fastest solution for a material considered to be waste. Therefore, following European Directive 2008/98/EC on waste, which sets out a hierarchy of priorities for waste treatment (prevention, reuse, recycling, other types of recovery and, finally, disposal), current membrane management is not coherent with the basic principles of European environmental legislation; hence, new less environmentally harmful handling alternatives are desired to move toward a circular economy system and to achieve a cross-continental recycling society (Darton and Fazel, 2001; European commission, 2008; Lawler et al., 2015; Siddique et al., 2008).

One of the main factors that affects RO membrane discarding is biofouling (Nguyen et al., 2012), a serious issue that compromises the membrane filtration process by shortening membrane service life (5-10 years) and raising its replacement rate (10-15% per year) (Darton and Fazel, 2001; Landaburu-Aguirre et al., 2016). Consequently, different alternatives have been proposed to extend the lifespan of discarded membranes. One such alternative is to recycle discarded RO membranes by removing the active polyamide (PA) layer, which is an interesting solution (Lawler et al., 2013). This transformation process is based on chemical modification using oxidant agents such as K_7MnO_4 and NaOCl which, under controlled conditions, convert EoL RO membranes into reusable nanofiltration (NF) or ultrafiltration (UF) membranes (Ambrosi and Tessaro, 2013; García-Pacheco et al., 2015; Raval et al., 2012). However, not all discarded RO membranes can be recycled and reused as pressure-driven membranes because the transformation success is dependent on the nature of PA (Do et al., 2012a, 2012b).

Membrane biofilm reactors (MBfRs) are an emerging membrane technology and have been recently used to overcome the growing need for treating poor quality water. To date, MBfRs have tested porous, dense and composite membranes (Martin et al., 2012). However, the role of the membrane in MBfRs differs from that in RO membranes and membrane bioreactors (MBRs) because they neither act as filters (Li and Zhang, 2018; Nerenberg, 2016, 2005), nor are they classical reactors as they provide new functions to surfaces, beyond that of mere supports material (Halan et al., 2012). MBfRs use gas-permeable membranes to remove pollutants from water by supplying electron donors or acceptors across the membrane, with the aim of enhancing the biological activity of the bacterial biofilm immobilized on the membrane (Li et al., 2008; Martin and Nerenberg, 2012; Syron and Casey, 2008; Zhou et al., 2019). Interestingly, companies such as APTwater, Inc. (Long Beach, CA, USA) have developed similar membrane configurations to RO units (Martin and Nerenberg, 2012). So even though membrane functions differ among these technologies, similar compositions and layouts can be used.

In previous studies, we proposed a novel recycling option for discarded RO membranes by converting them into low-cost thin-film composite support material for MBfRs (Morón-López et al., 2019). We proved that discarded RO membranes could be directly used as surfaces for immobilizing bacteria and carry out a desired reaction. Even we observed that the intrinsic fouling of discarded membranes may act as a conditioning agent and increase the bacterial deposition rate. In this manner, we linked the waste from pressure-driven membranes to MBfR technology for the first time. The biological activity of the biofilm generated on the discarded desalination membrane was proven

by removing microcystins (MC), a group of potent hepatotoxins produced by harmful cyanobacterial algal blooms (cyanoHABs) in eutrophic water (Buratti et al., 2017; Dawson, 1998; Lawton and Robertson, 1999). For this reason, although MBfRs have been successfully used to remove a wide variety of wastewater pollutants (Casey et al., 1999; Ontiveros-Valencia et al., 2018), we also demonstrated that our recycled membrane biofilm reactor (R-MBfR) is a suitable method to remove pollutants from surface water.

The present work attempted to go one step further by evaluating the effect of the transformation process through chlorination on discarded RO membranes. This process could be also interesting for recycling membranes into MBfRs due to both its simultaneous gas permeability enhancing, after partial or total removal of the polyamide (PA) layer, and the cleaning effect that chlorine may provide by removing the previous fouling, which is a conditioning agent but highly dependent from the water source used. However, the use of chlorine on the surfaces may also modify the membrane characteristics and consequently, the bacterial deposition. Therefore, this study is focused on investigate if: a) chlorination changes key surface characteristics for conditioning and bacterial association, such as previous fouling presence, charge, contact angle and surface roughness; b) the MC-degrading bacteria is able to attach on transformed surfaces and carry out the biological activity; c) the PA removal of the discarded membranes influences on gas permeability, adding value to the transformation process. All these newly acquired characteristics were compared with those already studied in untransformed discarded RO membranes in the previous work (Morón-López et al., 2019). So we provide new knowledge for

optimizing the R-MBfR concept by opening up new horizons for future membrane technology applications as part of circular economy principles.

2. Material and Method

2.1 Membranes and chemical reagents

Experiments were performed on the membranes obtained from EoL PA-TFC RO membranes. For this purpose, membrane coupons (216 cm^2) were taken from 8 inch-diameter spiral wound modules. The EoL membranes had originally been used for water desalination for more than 3 years and presented fouling of different natures. On the one hand, the TM 720-400 (*Toray*) module had treated brackish water (BW). On the other hand, the HSWC3 (*Hydranautics*) module had treated seawater (SW). The end-of-life RO membranes were transformed in recycled NF and UF membranes using two different dose level of NaOCl. All the membranes were conserved in Milli-Q water before being analyzed. NaOCl (10%) was purchased from Scharlab and used to transform the EoL RO membranes.

2.2. Transformation process of the EoL RO membranes

The EoL RO membranes were washed out with Milli-Q water, followed by exposing them to a dose level of 6,200 ppm·h and 300,000 ppm·h of NaOCl at pH 10, for 24 h at room temperature and under static conditions to obtain NF and UF membranes, respectively. These dose levels were selected based on the previous confirmation that they fell within a proper dose range for converting EoL RO membranes into NF and UF recycled membranes (García-Pacheco et al., 2015; Molina et al., 2018, 2015). Thus the obtained membranes were: BW transformed into NF (BWt-NF) and into UF (BWt-UF); SW transformed into NF

(SWt-NF) and UF (SWt-UF). After these transformation processes, coupons were taken out of the containers and thoroughly washed with Milli-Q water until a pure water pH was accomplished. For comparison purposes, the same non transformed type membranes (BWd and SWd) were also included (Morón-López et al., 2019). All the membranes are kept in Milli-Q water until used.

2.3. Membrane surface characterization

Similar experimental set-up and analyzing methodology to our previous work were performed in order to compare with discarded untransformed membranes results (Morón-López et al., 2019). For membrane characterization, all the membranes were previously dried at 100 ºC for 24 h to avoid the interaction of occluded water.

2.3.1. *Zeta potential measurements*

A Surface Zeta Potential Cell (ZEN 1020, Malvern) was employed to measure the surface Zeta potential via electrophoretic light scattering (Zetasizer Nano ZS), under the same conditions applied in previous studies (Morón-López et al., 2019; Santiago-Morales et al., 2016).

2.3.2. *Contact angle measurement*

Surface wettability tests were performed by a static contact angle meter via the sessile drop technique in a KSV CAM200 instrument (KSV Instruments, USA), under identical conditions as in previous studies (Molina et al., 2015; Morón-López et al., 2019).

2.3.3. *Atomic-force microscopy (AFM)*

Following the same experimental conditions of previous works (Molina et al., 2018; Morón-López et al., 2019), atomic-force microscopy (AFM) experiments

for the roughness analysis were carried out in the tapping mode by a Multimode AFM (Vecco Instruments, Santa Barbara, CA, USA), equipped with a Nanoscope Iva control system (software version 6.14r1).

2.4. Bacterial deposition test

MC-degrading bacteria *Sphingopyxis* sp. strain IM-1 has been proven to efficiently degrade the MC molecule until small peptides and amino acids (Jones et al., 1994; Lezcano et al., 2016). For this reason, this strain was selected to analyze its attachment to membranes BWt-NF, BWt-UF, SWt-NF and SWt-UF. The bacterial growth on tested membranes was performed by following the steps previously described (Morón-López et al., 2019). Then, samples were analyzed by confocal laser scanning microscopy (CLSM) and scanning electron microscopy (SEM). The negative controls without strain IM-1 were also performed for the comparisons.

2.5. Confocal laser scanning microscopy (CLSM)

The bacterial coverage images were obtained with a confocal laser scanning microscope (CLSM Leica SP5, Leica Microsystems), using the same experimental conditions reported in a previous study (Morón-López et al., 2019). The bacterial coverage percent (%) on the transformed membrane surfaces was analyzed by the ImageJ software (Abràmoff et al., 2004).

2.6. Scanning electron microscopy (SEM)

Several imaging devices have been used. The first (XL30 ESEM Model (Phillips)) was used to observe the cross-section of membranes. For this purpose, membranes were broken properly after being frozen in liquid nitrogen.

Samples were dried and then gold-sputtered with a Sputter Coater Polaron SC7640 model to achieve a 13-15 nm thickness prior to the SEM analysis. Second, two other SEMs were employed to examine the surfaces of the membranes. The transformed membrane surfaces were observed by an S-8000 Model (Hitachi) device. A SEM Zeiss DSM 950 (Germany) was used to observe the bacterial attachment of BWt-NF after the bacterial deposition test, following the steps previously reported (Morón-López et al., 2019).

2.7. *MC degradation test*

Toxins were obtained by extracting the fresh cyanobacterial scum collected from natural water (Lezcano et al., 2016). The MC mixture was composed of different variants: 84.5% of –LR; 9.86 % of -RR and 5.64 of -YR.

Having completed the bacterial deposition test, we chose the membrane with the highest bacterial coverage for the MC degradation test. After growing the MC-degrading bacteria, the MC degradation test of selected membrane was performed under the same experimental conditions previously reported (Morón-López et al., 2019). The controls with the same membrane and conditions, but no bacteria, were also analyzed.

According to the reference (Morón-López et al., 2017), an HPLC-MS-TOF (Agilent 6230 accurate mass TOF Agilent Technologies, Santa Clara, CA, USA) was used to quantify the MC concentration. After that, the MC degradation kinetics of the bacteria attached to the transformed membrane was calculated following previous works (Li et al., 2014; Xu et al., 2011). Because of a lag phase was observed, calculates for determining *k* constant were done taking the first point at which biodegradation began (Ho et al., 2012).

247 *2.8. Gas permeability test*

248 The air permeability of the studied membranes was investigated with an MBfR
249 cell by measuring the air flow across the membrane by a bubble flowmeter at
250 room temperature and pressure at 1 bar. For the permeability calculations, a 0.2
251 μm membrane thickness was taken into account for the discarded and
252 transformed NF types, while the thickness of the transformed UF was 50, and
253 was 30 μm for the BW model and the SW model, respectively. All the
254 membranes measurements were taken in triplicate using different parts of the
255 membrane coupons. Given the dissimilar ways to show the gas permeability of
256 the membranes found in the literature, air permeability was calculated in
257 $Ncm^3 \cdot cm \cdot cm^{-2} \cdot s^{-1} \cdot cmHg^{-1}$ (Barrers) and air flux in $Ncm^3 \cdot cm^{-2} \cdot s^{-1} \cdot cmHg^{-1}$ (J).
258 Additionally, to provide more information of tested membranes for other
259 hypothetical applications, the pure hydrogen permeability was also tested
260 following the same steps and criteria commented above.

261 *2.9. Data analysis*

262 Statistical analyses were conducted using the Statistical Package for Social
263 Sciences (SPSS, Inc.) software, v.17. Normality and homogeneity of variances
264 were performed using the Shapiro-Wilk and Levene tests, respectively. To
265 determine significant differences between bacterial coverage and zeta potential
266 a one-way analysis of variance (ANOVA) and a Turkey HSD analysis were run.
267 One-way ANOVA and Tamhane *post hoc* analyses were performed for
268 remaining variables with non-homogeneous variances.

269 **3. Results and discussion**

3.1. *Characterization of the transformed EoL RO membranes*

The membranes used in this study were EoL RO polyamide thin film composite (PA-TFC) membranes because of many existing discarded modules (Geise et al., 2010). PA-TFC membranes are composed for a three-layer structure, typically based on a non-woven fibrous support, a porous polysulfone (PSF) sublayer and a dense polyamide (PA) ultrathin surface. To transform the EoL discarded membranes, which came from treating brackish water (BWd type) and seawater (SWd type), we chemically attacked the membrane surface with NaOCl. This process removes not only previously attached fouling, but also the PA layer in a controlled manner to obtain transformed NF and UF membranes (BWt-NF, BWt-UF, SWt-NF and SWt-UF types) from the discarded types (Kwon and Leckie, 2006; Rodríguez et al., 2002).

The chemical attack with 6,200 ppm·h of NaOCl partially removed the PA layer, and BWt-NF and SWt-NF membranes were obtained (Fig. 1). Conversely with the BWt-UF and SWt-UF membranes obtained after treating them with 300,000 ppm·h of NaOCl, PA removal was total, and a porous surface which belonged to the PSF layer was observed. In both cases, a cleaning effect was achieved and no fouling was noted. These results agree with authors who generated recycled NF and UF membranes using the same NaOCl doses in previous works (García-Pacheco et al., 2015; Molina et al., 2018).

The transformation process by chlorination also modifies key surface characteristics for bacterial attachment, such as charges, hydrophobicity and roughness (Table 1). Zeta potential measurements showed a negatively charged surface after chlorine attack on all surfaces, as in other studies (Do et

al., 2012a; Kwon and Leckie, 2006; Xu et al., 2013). Contact angle changes were also observed after chlorine transformation. The transformed membranes that belonged to the SW model were more hydrophobic than those for the BW model, and the most hydrophilic surface was observed in BWt-NF. These results agree with studies in which the incorporation of chlorine onto the surface led to greater hydrophobicity (Kwon and Leckie, 2006; Simon et al., 2009), while other studies have shown that chlorine attack triggers hydrophilic surfaces (Do et al., 2012a; Molina et al., 2018). Besides, fouling removal seems to more strongly affect the contact angle of the SW model, possibly due to its more organic nature (Morón-López et al., 2019).

In spite of changes in the aforementioned properties, the most obvious surface alteration between membrane types was roughness (Table 1, Fig. 2). Average roughness (R_a, the average deviation of the peaks and valleys from the mean height) and root mean square roughness (R_q, standard deviation of the peaks and valleys) showed that the roughness of both membrane models significantly decreased at higher chlorine doses (BWt-UF and SWt-UF). This significant drop in roughness could be due to the PA layer being removed (Al-Jeshi and Neville, 2006; Jiang et al., 2018; Molina et al., 2018). The fact that roughness remained similar for BWt-NF and BWd, but significantly lowered more in SWt-NF than SWd, was remarkable, and agrees with the works which have indicated that modification by chlorination is PA nature-dependent (Do et al., 2012b; Molina et al., 2015). It also suggests that fouling nature triggers more roughness on SWd than BWd and, hence, its removal affects SWd roughness more.

3.2. *Conditioning and bacterial attachment*

A biofilm is referred to as a surface-associated microbial community enclosed by extracellular polymeric substances (EPS). Biofilm development is a complex process whose stages comprise a first substratum conditioning, initial bacterial attachment, following by biofilm formation and bacterial dispersion when biofilm matures (Characklis and Cooksey, 1983). In order to identify if the transformation process affected to conditioning and bacterial deposition, and therefore for biofilm formation, we focused on early, but no less important, stages where the surface plays a relevant role (Fig. 3). For this purpose, we immersed the transformed membranes into a culture of MC-degrading bacteria *Sphingopyxis* sp. strain IM-1. Worth mentioning that although MBfRs are composed of multi-species biofilms, the MC degradation capacity has been confined to limited number of species so far (Li et al., 2017). For this reason, as well as to avoid possible interferences in biological activity interpretation due to interactions between microorganisms, we have used single specie as MC-degrading biofilm. Additionally, because of the cell deposition is dependent of interaction between cells and surfaces (Donlan, 2002), we also included Calcium (Ca^{2+}) as a *quorum-sensing* molecule and a surface conditioner (He et al., 2016; Li and Elimelech, 2004; Mangwani et al., 2014).

Unlike the untransformed discarded membranes, the cleaning of the surface during the transformation process could lead to direct interaction between Ca^{2+} and the dissolved nutrients with the surface without fouling, as outlined in Figure 3. We observed that the BWt-NF membrane was the only membrane favorable for conditioning, and showed the best bacterial attachment in the CLMS images (Fig. 4). This membrane presented a similar roughness, but a smaller contact angle, than SWt-NF. Hence, hydrophilicity could be considered the beneficial

343 factor for bacterial attachment because water-miscible conditioners have better
344 access of to the surface (Characklis and Wilderer, 1989; Hou et al., 2013).
345 Unlike SWt-NF, BWt-UF and SWt-UF did not show any bacterial deposition,
346 possibly due to their drastic decrease in roughness, and also to the
347 hydrophobicity of their surfaces. Even the least negative charge of BWt-UF
348 could affect its low bacterial coverage as a result of its minor attraction to Ca^{2+}
349 and other nutritive substances (Fang et al., 2018). All these results agree with
350 other studies in which hydrophilic and roughness surfaces enhanced bacterial
351 deposition (Chen et al., 2013; Guo et al., 2013; Subramani et al., 2009). They
352 are also consistent with those authors who conclude that not all cultures
353 successfully colonize certain membrane types (Rothemund et al., 1996).

354 Compared to the untransformed discarded membranes, the amount of bacterial
355 attached to the BWt-NF surface was significantly higher than BWd and similar
356 to SWd (Fig. 4). Therefore, these results suggest that, at certain doses of
357 NaOCl, the chlorination process could simultaneously remove fouling and
358 improve the key surface characteristics for conditioning and bacterial deposition
359 in some membranes (Fig. 3). Chlorine could interact with certain types of PAs to
360 result in a more hydrophilic active-charged surface for Ca^{2+} and nutrient
361 absorption (Herzberg et al., 2009; Li and Elimelech, 2004). In this manner,
362 transforming discarded membranes could be advantageous for avoiding the
363 highly variable fouling nature of untransformed discarded types, which could be
364 relevant to establish a hypothetical methodology of recycling. On the other
365 hand, in reference to the worst results obtained in remaining membranes, it
366 should be noted that this prior conditioning to the initial bacterial attachment
367 could also modify these properties with time (Jin et al., 2009; Zhao et al., 2015).

Hence, mid- and long-term studies are necessary to confirm the rejection of some membrane types for biofilm formation.

3.3. *MC degradation capability*

Once the strain IM-1 was attached to the transformed surfaces in BWt-NF, an MC degradation test was run to observe if the chlorine modifications affected its biological activity. Figure 5.1 shows that, after an acclimation time in the presence of the toxin, strain IM-1 was able to remove the total MC concentration (1 $mg \cdot L^{-1}$) in 6 h. Besides, no MC removal was observed in the negative control without bacteria (Fig. 5.1 and 5.2.b), which indicates that MC degradation was biologically-mediated. The MC degradation kinetics follows the pseudo-first order model, where k and $T_{1/2}$ agree with those obtained previously with untransformed discarded membranes (Morón-López et al., 2019). Therefore, it could be concluded that the chemical modification during the transformation process maintains viable conditions for biological reactions in certain EoL membranes. Nonetheless, we also highlighted that the potential use of membranes transformed into MBfRs would still be less appealing than using untransformed discarded membranes due to the environmental impacts derived from the transformation process (Nguyen et al., 2012). Consequently, further experiments and techno-economic and environmental analysis are needed to clarify the advantages and disadvantages of transforming discarded membranes in larger scales.

3.4. *Gas permeability*

One of the most crucial aspects in MBfRs is membrane typology due to differences in each membrane's gas transfer properties (Li et al., 2008;

Nerenberg, 2016; Syron and Casey, 2008; Tang et al., 2012). The gas transfer resistance of these membranes depends on the material's character and thickness. Porous membranes provide high gas transfer rates given the faster gaseous diffusion in gas-filled pores (Semmens, 2005). However, drawbacks such as a low bubble point, clogging and wetting are some of the limitations of porous materials (Casey et al., 1999). Conversely, dense membranes are free of clogging and wetting, but their gas transfer is lower than porous membranes because gas is firstly dissolved through the membrane's material. To overcome this diffusion resistance, dense membranes work at high intermembrane pressure. As an alternative, a thinner dense layer achieves less mass resistance. Hence, composite membranes offer a promising, but more expensive, option than others (Martin and Nerenberg, 2012).

Using recycled desalination composite membranes for MBfRs could be an interesting low-cost option to achieve the desired throughputs. To study if the untransformed and transformed membranes allowed gas permeability, we investigated air permeability before and after dense PA layer removal. As shown in Table 2, all tested membranes were able to offer air flux at low pressure. Consequently, up to our knowledge, we proved for first time that membranes originally manufactured for desalination purposes are capable of diffusing gases from the inner non-woven fibrous layer. In addition, unequally fluxes were obtaining depending on the chlorine doses used during the transformation process. The PSF porous BWt-UF and SWt-UF have an air permeability that is between two and three orders of magnitude higher than the untransformed discarded membranes and those transformed into NF. Conversely, similar air permeability was observed between the untransformed

417 discarded membranes and those transformed into NF. Therefore, as expected,
418 our results suggested that total PA removal from discarded membranes would
419 lead to higher air permeability. However, no increase of gas permeability is
420 achieved at doses levels of 6,200 ppm·h of NaOCl. Besides, our results also
421 indicated higher air permeability in the BW model than in the SW model. This
422 could be due to the difference in selective layer thickness. Figure 1 shows the
423 cross-section micrographs of the PSF layer in the transformed membranes. The
424 thickness of the recycled membranes used originally as the RO BW membranes
425 almost doubled those which treated seawater. This variation in thickness could
426 be due to differences in membrane compaction, as BW membranes have been
427 subjected to lower pressure than SW membranes during their previous service
428 times in desalination plants (Molina et al., 2018).

429 When comparing the air permeability of the tested membranes with the
430 membranes made especially for gas transfer from studies based on MBfRs, we
431 obtained promising results. We observed that SWd and SWt-NF were of the
432 same order of magnitude as the commercial polyethylene composite membrane
433 used by (Ahmed et al., 2004), while the BWd and BWt-NF membranes were
434 160-fold more permeable. The composite polyolefin membrane of (Motlagh et
435 al., 2008), and that commercialized for air separation made of Teflon of
436 Cerqueira et al., (2013), showed an oxygen flux of $3.00 \cdot 10^{-5}$ and $4.91 \cdot 10^{-4}$
437 $Ncm^3 \cdot cm^{-2} \cdot s^{-1} \cdot cmHg^{-1}$, respectively. Otherwise, the comparison made of the
438 polyurethane composite membranes by Tang et al., (2012) displayed lower
439 oxygen fluxes than previous references. Therefore, our recycled composite
440 membranes were far more permeable than those in other studies, which
441 suggests that these membranes could be a green low-cost alternative for

MBfRs. Worth mentioning that pure hydrogen permeability of these membranes was also tested (Table S1) and the hydrogen fluxes obtained were higher than those composite membranes permeabilities reported by Tang et al., (2012). Accordingly, although the hydrogen application is not required for removing MC by an aerobic biofilm, our preliminary data suggest that recycled membranes could also be appropriate for other uses of hydrogen-based MBfRs.

By focusing on transformed to porous membranes (BWt-UF and SWt-UF), the total PA removal also provided higher air fluxes than those of the aforementioned composite membranes. However, when compared with the oxygen permeabilities of the other porous materials used in MBfRs, such as polyethylene ($8.00 \cdot 10^{-1}$ Barrers), polypropylene ($2.00 \cdot 10^{-1}$ Barrers), polyvinyl chloride ($1.40 \cdot 10^{-2}$ Barrers), polyvinyl alcohol ($1.00 \cdot 10^{-2}$ Barrers) and polyvinylidene fluoride ($3.00 \cdot 10^{-3}$ Barrers), our porous membranes were less permeable by several orders of magnitude (Cote, 1989; Hou et al., 2013). These results could be due to the nature of the PSF of the transformed membranes. Therefore, by taking into account the possible environmental impact and minor bacterial deposition rate, the transformation process done to UF membranes for MBfRs did not seem to provide any added value. Nonetheless, BWt-NF is especially interesting because the transformation into NF cleaned the surfaces and improved the conditioning and bacterial attachment, maintaining a competitive gas permeability regarding to the aforementioned studies. The thin film dense PA layer of the composite discarded RO membranes could supply competitive bubbleless aeration with low mass resistance, providing a low-cost alternative for MBfRs. Therefore, as is schematically illustrated in Fig. 6, this gas permeability could benefits the

biological activity of the biofilms thanks to the high oxygenic-surface provided, which would enhance the pollutant removal, such as MC, by R-MBfRs.

4. Conclusion

This work provides new findings for recycling the huge amount of EoL RO desalination membrane for MBfRs. We prove that chlorination process of certain discarded membranes could be beneficial for removing previous fouling and enhancing the attachment of the desired bacteria. This is of interest to make the membrane recycling totally independent of previous fouling nature, which is important to establish a hypothetical process of membrane recycling for MBfR. Besides, the chlorination process of the BWt-NF did not affect to the MC degradation of the attached strain IM-1; hence, this chemical modification does not have a negative effect for later biological activity. On the other hand, our results also demonstrate that PA-TFC membranes originally manufactured for desalination purposes are capable to allow gases fluxes at low pressures, which is an essential property of MBfRs. Promising outcome is shown by the composite typology in BWt-NF due to display higher air permeabilities than other composite membranes reported in the literature, together with meeting the rest of properties for biofilm developments. Therefore, the current work gives further evidence of the potential of recycling discarded desalination membranes for R-MBfRs, offering a solution for poor quality water treatments and following circular economy principles.

Acknowledgements

The financial support provided by the Spanish Ministry of Science and Innovation through project INREMEM (CTM2015-65348-C2-1-R) is gratefully acknowledged.

The biofilm visualization has been performed by ICTS “NANBIOSIS”, more specifically by the Confocal Microscopy Service: Ciber in Bioengineering, Biomaterials & Nanomedicine (CIBER-BNN) at the Alcala University (CAI Medicine Biology).

Compliance with ethical standards

Conflict of interest

The authors declare that they have no conflict of interest.

References

Abràmoff, M.D., Magalhães, P.J., Ram, S.J., 2004. Image processing with imageJ. Biophotonics Int. 11, 36–41. doi:10.1117/1.3589100

Ahmed, T., Semmens, M.J., Voss, M.A., 2004. Oxygen transfer characteristics of hollow-fiber, composite membranes. Adv. Environ. Res. 8, 637–646. doi:10.1016/S1093-0191(03)00036-4

Al-Jeshi, S., Neville, A., 2006. An investigation into the relationship between flux and roughness on RO membranes using scanning probe microscopy. Desalination 189, 221–228. doi:10.1016/j.desal.2005.08.001

Ambrosi, A., Tessaro, I.C., 2013. Study on Potassium Permanganate Chemical Treatment of Discarded Reverse Osmosis Membranes Aiming their Reuse. Sep. Sci. Technol. 48, 1537–1543. doi:10.1080/01496395.2012.745876

Buratti, F.M., Manganelli, M., Vichi, S., Stefanelli, M., Scardala, S., Testai, E.,

512 Funari, E., 2017. Cyanotoxins: producing organisms, occurrence, toxicity,
513 mechanism of action and human health toxicological risk evaluation. Arch.
514 Toxicol. 91, 1049–1130. doi:10.1007/s00204-016-1913-6
515 Casey, E., Glennon, B., Hamer, G., 1999. Review of membrane aerated biofilm
516 reactors. Resour. Conserv. Recycl. 27, 203–215. doi:10.1016/S0921-
517 3449(99)00007-5
518 Cerqueira, A.C., Nobrega, R., Jr, G.L.S.A., Dezotti, M., 2013. Oxygen air
519 enrichment through composite membranes: Application to an Aerated
520 Biofilm Reactor 30, 771–779.
521 Characklis, W.G., Cooksey, K.E., 1983. Biofilms and Microbial Fouling,
522 Advances in Applied Microbiology. doi:10.1016/S0065-2164(08)70355-1
523 Characklis, W.G., Wilderer, P.A., 1989. Structure and Function of Biofilms 436.
524 Chen, Y.P., Zhang, P., Guo, J.S., Fang, F., Gao, X., Li, C., 2013. Functional
525 groups characteristics of EPS in biofilm growing on different carriers.
526 Chemosphere 92, 633–638. doi:10.1016/j.chemosphere.2013.01.059
527 Cote, P., 1989. Bubble-free aeration transfer analysis. J. Memb. Sci. 47, 91–
528 106.
529 Darton, E., Fazel, M., 2001. A statistical review of 150 membrane autopsies.
530 62nd Annu. Int. Water Conf. ….
531 Dawson, R.M., 1998. The toxicology of microcystins. Toxicon 36, 953–962.
532 doi:10.1016/S0041-0101(97)00102-5
533 Do, V.T., Tang, C.Y., Reinhard, M., Leckie, J.O., 2012a. Effects of hypochlorous
534 acid exposure on the rejection of salt, polyethylene glycols, boron and
535 arsenic(V) by nanofiltration and reverse osmosis membranes. Water Res.
536 46, 5217–5223. doi:10.1016/j.watres.2012.06.044

537 Do, V.T., Tang, C.Y., Reinhard, M., Leckie, J.O., 2012b. Degradation of
538 polyamide nanofiltration and reverse osmosis membranes by hypochlorite.
539 Environ. Sci. Technol. 46, 852–859. doi:10.1021/es203090y
540 Donlan, R.M., 2002. Biofilms: microbial life on surfaces. Emerg Infect Diseases.
541 http://www.cdc.gov/ncidod/EID/vol8no9/02-0063.htm 8, 881–890.
542 doi:10.3201/eid0809.020063
543 Ercin, A.E., Hoekstra, A.Y., 2014. Water footprint scenarios for 2050: A global
544 analysis. Environ. Int. 64, 71–82. doi:10.1016/j.envint.2013.11.019
545 European commission, 2008. 19.11.2008.
546 Fang, C., Sun, J., Zhang, B., Sun, Y., Zhu, L., Matsuyama, H., 2018.
547 Preparation of positively charged composite nanofiltration membranes by
548 quaternization crosslinking for precise molecular and ionic separations. J.
549 Colloid Interface Sci. 531, 168–180. doi:10.1016/j.jcis.2018.07.034
550 García-Pacheco, R., Landaburu-Aguirre, J., Molina, S., Rodríguez-Sáez, L.,
551 Teli, S.B., García-Calvo, E., 2015. Transformation of end-of-life RO
552 membranes into NF and UF membranes: Evaluation of membrane
553 performance. J. Memb. Sci. 495, 305–315.
554 doi:10.1016/j.memsci.2015.08.025
555 Geise, G.M., Lee, H.-S., Miller, D.J., Freeman, B.D., Mcgrath, J.E., Paul, D.R.,
556 2010. Effect of MolecularWeight and Temperature on Physical Aging of
557 ThinGlassy Poly(2,6-dimethyl-1,4-phenylene oxide) Films. J. Polym. Sci.
558 Part B Polym. Phys. 45, 1390–1398. doi:10.1002/polb
559 Guo, K., Freguia, S., Dennis, P.G., Chen, X., Donose, B.C., Keller, J., Gooding,
560 J.J., Rabaey, K., 2013. Effects of surface charge and hydrophobicity on
561 anodic biofilm formation, community composition, and current generation in

562 bioelectrochemical systems. Environ. Sci. Technol. 47, 7563–7570.
563 doi:10.1021/es400901u
564 Halan, B., Buehler, K., Schmid, A., 2012. Biofilms as living catalysts in
565 continuous chemical syntheses. Trends Biotechnol. 30, 453–465.
566 doi:10.1016/j.tibtech.2012.05.003
567 He, X., Wang, J., Abdoli, L., Li, H., 2016. Mg2+/Ca2+ promotes the adhesion of
568 marine bacteria and algae and enhances following biofilm formation in
569 artificial seawater. Colloids Surfaces B Biointerfaces 146, 289–295.
570 doi:10.1016/j.colsurfb.2016.06.029
571 Herzberg, M., Kang, S., Elimelech, M., 2009. Role of Extracellular Polymeric
572 Substances (EPS) in Biofouling of Reverse Osmosis Membranes. Environ.
573 Sci. Technol. 43, 4393–4398. doi:10.1021/es900087j
574 Ho, L., Tang, T., Hoefel, D., Vigneswaran, B., 2012. Determination of rate
575 constants and half-lives for the simultaneous biodegradation of several
576 cyanobacterial metabolites in Australian source waters. Water Res. 46,
577 5735–5746. doi:10.1016/j.watres.2012.08.003
578 Hou, F., Li, B., Xing, M., Wang, Q., Hu, L., Wang, S., 2013. Surface modification
579 of PVDF hollow fiber membrane and its application in membrane aerated
580 biofilm reactor (MABR). Bioresour. Technol. 140, 1–9.
581 doi:10.1016/j.biortech.2013.04.056
582 Jiang, B., Zhang, N., Zhang, L., Sun, Y., Huang, Z., Wang, B., Dou, H., Guan,
583 H., 2018. Enhanced separation performance of PES ultrafiltration
584 membranes by imidazole-based deep eutectic solvents as novel functional
585 additives. J. Memb. Sci. 564, 247–258. doi:10.1016/j.memsci.2018.07.034
586 Jin, X., Huang, X., Hoek, E.M. V, 2009. Role of specific ion interactions in

587 seawater RO membrane fouling by alginic acid. Environ. Sci. Technol. 43,
588 3580–3587. doi:10.1021/es8036498
589 Jones, G.J., Bourne, D.G., Blakeley, R.L., Doelle, H., 1994. Degradation of the
590 Cyanobacterial Hepatotoxin Microcystin by Aquatic Bacteria. Nat. Toxins 2,
591 228–235.
592 Kwon, Y.N., Leckie, J.O., 2006. Hypochlorite degradation of crosslinked
593 polyamide membranes. II. Changes in hydrogen bonding behavior and
594 performance. J. Memb. Sci. 282, 456–464.
595 doi:10.1016/j.memsci.2006.06.004
596 Landaburu-Aguirre, J., García-Pacheco, R., Molina, S., Rodríguez-Sáez, L.,
597 Rabadan, J., García-Calvo, E., 2016. Fouling prevention, preparing for re-
598 use and membrane recycling. Towards circular economy in RO
599 desalination. Desalination 393, 16–30. doi:10.1016/j.desal.2016.04.002
600 Lawler, W., Alvarez-Gaitan, J., Leslie, G., Le-Clech, P., 2015. Comparative life
601 cycle assessment of end-of-life options for reverse osmosis membranes.
602 Desalination 357, 45–54. doi:10.1016/j.desal.2014.10.013
603 Lawler, W., Antony, A., Cran, M., Duke, M., Leslie, G., Le-Clech, P., 2013.
604 Production and characterisation of UF membranes by chemical conversion
605 of used RO membranes. J. Memb. Sci. 447, 203–211.
606 doi:10.1016/j.memsci.2013.07.015
607 Lawton, L. a., Robertson, P.K.J., 1999. Physico-chemical treatment methods for
608 the removal of microcystins (cyanobacterial hepatotoxins) from potable
609 waters. Chem. Soc. Rev. 28, 217–224. doi:10.1039/a805416i
610 Lezcano, M.Á., Morón-López, J., Agha, R., López-Heras, I., Nozal, L., Quesada,
611 A., El-Shehawy, R., 2016. Presence or absence of mlr genes and nutrient

612 concentrations co-determine the microcystin biodegradation efficiency of a
613 natural bacterial community. Toxins (Basel). 8. doi:10.3390/toxins8110318
614 Li, J., Li, R., Li, J., 2017. Current research scenario for microcystins
615 biodegradation – A review on fundamental knowledge, application
616 prospects and challenges. Sci. Total Environ. 595, 615–632.
617 doi:10.1016/j.scitotenv.2017.03.285
618 Li, J., Peng, L., Li, J., Qiao, Y., 2014. Divergent responses of functional gene
619 expression to various nutrient conditions during microcystin-LR
620 biodegradation by Novosphingobium sp. THN1 strain. Bioresour. Technol.
621 156, 335–341. doi:10.1016/j.biortech.2013.12.118
622 Li, Q., Elimelech, M., 2004. Organic fouling and chemical cleaning of
623 nanofiltration membranes: Measurements and mechanisms. Environ. Sci.
624 Technol. 38, 4683–4693. doi:10.1021/es0354162
625 Li, T., Liu, J., Bai, R., 2008. Membrane aerated biofilm reactors: a brief current
626 review. Recent Pat. Biotechnol. 2, 88–93.
627 doi:10.2174/187220808784619739
628 Li, Y., Zhang, K., 2018. Pilot scale treatment of polluted surface waters using
629 membrane-aerated biofilm reactor (MABR). Biotechnol. Biotechnol. Equip.
630 32, 376–386. doi:10.1080/13102818.2017.1399826
631 M.Mekonnen, M., Hoekstra, Y.A., 2016. Four Billion People Experience Water
632 Scarcity. Sci. Adv. 2, 1–7. doi:10.1126/sciadv.1500323
633 Mangwani, N., Shukla, S.K., Rao, T.S., Das, S., 2014. Calcium-mediated
634 modulation of Pseudomonas mendocina NR802 biofilm influences the
635 phenanthrene degradation. Colloids Surfaces B Biointerfaces 114, 301–
636 309. doi:10.1016/j.colsurfb.2013.10.003

637 Martin, K.J., Boltz, J.P., Nerenberg, R., 2012. The Membrane Biofilm Reactor
638 (MBfR) for Wastewater Treatment: Applications, Design Considerations,
639 and Technology Outlook. Proc. Water Environ. Fed. 2012, 4032–4044.
640 doi:10.2175/193864712811708347
641 Martin, K.J., Nerenberg, R., 2012. The membrane biofilm reactor (MBfR) for
642 water and wastewater treatment: Principles, applications, and recent
643 developments. Bioresour. Technol. 122, 83–94.
644 doi:10.1016/j.biortech.2012.02.110
645 Molina, S., García Pacheco, R., Rodríaguez Sáez, L., García-Calvo, E.,
646 Campos Pozuelo, E., Zarco Martínez, D., González de la Campa, J., De
647 Abajo González, J., 2015. Transformation of end-of-life RO membrane into
648 recycled NF and UF membranes, surface characterization, in: The
649 International Desalination Association World Congress on Desalination and
650 Water Reuse. p. 20.
651 Molina, S., Landaburu-Aguirre, J., Rodríguez-Sáez, L., García-Pacheco, R., de
652 la Campa, J.G., García-Calvo, E., 2018. Effect of sodium hypochlorite
653 exposure on polysulfone recycled UF membranes and their surface
654 characterization. Polym. Degrad. Stab. 150, 46–56.
655 doi:10.1016/j.polymdegradstab.2018.02.012
656 Morón-López, J., Nieto-Reyes, L., El-Shehawy, R., 2017. Assessment of the
657 influence of key abiotic factors on the alternative microcystin degradation
658 pathway(s) (mlr −): A detailed comparison with the mlr route (mlr +). Sci.
659 Total Environ. 599–600, 1945–1953. doi:10.1016/j.scitotenv.2017.04.042
660 Morón-López, J., Nieto-Reyes, L., Senán-Salinas, J., Molina, S., El-Shehawy,
661 R., 2019. Recycled desalination membranes as a support material for

biofilm development: A new approach for microcystin removal during water treatment. Sci. Total Environ. 647, 785–793. doi:10.1016/j.scitotenv.2018.07.435

Motlagh, A.R.A., LaPara, T.M., Semmens, M.J., 2008. Ammonium removal in advective-flow membrane-aerated biofilm reactors (AF-MABRs). J. Memb. Sci. 319, 76–81. doi:10.1016/j.memsci.2008.03.020

Nerenberg, R., 2016. The membrane-biofilm reactor (MBfR) as a counter-diffusional biofilm process. Curr. Opin. Biotechnol. 38, 131–136. doi:10.1016/j.copbio.2016.01.015

Nerenberg, R., 2005. Membrane Biofilm Reactors for Water and Wastewater Treatment. A Semin. Adv. Water Wastewater Treat. 1–20.

Nguyen, T., Roddick, F.A., Fan, L., 2012. Biofouling of water treatment membranes: A review of the underlying causes, monitoring techniques and control measures. Membranes (Basel). 2, 804–840. doi:10.3390/membranes2040804

Ontiveros-Valencia, A., Zhou, C., Zhao, H., Tang, Y., Rittmann, B.E., 2018. Managing microbial communities in membrane biofilm reactors. Appl. Microbiol. Biotechnol. 9003–9014.

Paerl, H.W., Paul, V.J., 2012. Climate change: Links to global expansion of harmful cyanobacteria. Water Res. 46, 1349–1363. doi:10.1016/j.watres.2011.08.002

Peng Lee, K., C. Arnot, T., Mattia, D., 2011. A Review of Reverse Osmosis Membrane Materials for Desalination – Development to date and Future Potential. Authors 51, 32–37.

Raval, H.D., Chauhan, V.R., Raval, A.H., Mishra, S., 2012. Rejuvenation of

687 discarded RO membrane for new applications. Desalin. Water Treat. 48,
688 349–359. doi:10.1080/19443994.2012.704727
689 Rodríguez, J.J., Jiménez, V., Trujillo, O., Veza, J., 2002. Reuse of reverse
690 osmosis membranes in advanced wastewater treatment. Desalination 150,
691 219–225. doi:10.1016/S0011-9164(02)00977-3
692 Rothemund, C., Amann, R., Klugbauer, S., Manz, W., Bieber, C., Schleifer,
693 K.H., Wilderer, P., 1996. Microflora of 2,4-dichlorophenoxyacetic acid
694 degrading biofilms on gas permeable membranes. Syst. Appl. Microbiol.
695 19, 608–615. doi:10.1016/S0723-2020(96)80033-6
696 Santiago-Morales, J., Amariei, G., Letón, P., Rosal, R., 2016. Antimicrobial
697 activity of poly(vinyl alcohol)-poly(acrylic acid) electrospun nanofibers.
698 Colloids Surfaces B Biointerfaces 146, 144–151.
699 doi:10.1016/j.colsurfb.2016.04.052
700 Semmens, M.J., 2005. Membrane Technology: Pilot Studies of Membrane-
701 Aerated Bioreactors. Water Environment Research Foundation, Alexandria.
702 doi:10.2166/9781843397045
703 Siddique, R., Khatib, J., Kaur, I., 2008. Use of recycled plastic in concrete: A
704 review. Waste Manag. 28, 1835–1852. doi:10.1016/j.wasman.2007.09.011
705 Simon, A., Nghiem, L.D., Le-Clech, P., Khan, S.J., Drewes, J.E., 2009. Effects
706 of membrane degradation on the removal of pharmaceutically active
707 compounds (PhACs) by NF/RO filtration processes. J. Memb. Sci. 340, 16–
708 25. doi:10.1016/j.memsci.2009.05.005
709 Subramani, A., Huang, X., Hoek, E.M. V, 2009. Direct observation of bacterial
710 deposition onto clean and organic-fouled polyamide membranes. J. Colloid
711 Interface Sci. 336, 13–20. doi:10.1016/j.jcis.2009.03.063

712 Syron, E., Casey, E., 2008. Membrane-aerated biofilms for high rate
713 biotreatment: Performance appraisal, engineering principles, scale-up, and
714 development requirements. Environ. Sci. Technol. 42, 1833–1844.
715 doi:10.1021/es0719428
716 Tang, Y., Zhou, C., Van Ginkel, S.W., Ontiveros-Valencia, A., Shin, J.,
717 Rittmann, B.E., 2012. Hydrogen permeability of the hollow fibers used in
718 H2-based membrane biofilm reactors. J. Memb. Sci. 407–408, 176–183.
719 doi:10.1016/j.memsci.2012.03.040
720 Van Der Bruggen, B., Vandecasteele, C., Gestel, T. Van, Doyenb, W., Leysenb,
721 R., 2003. Review of Pressure-Driven Membrane Processes. Environ. Prog.
722 22, 46–56. doi:10.1002/ep.670220116
723 Vörösmarty, C.J., Green;, P., Salisbury;, J., Lammers, R.B., 2000. Global Water
724 Resources: Vulnerability from Climate Change and Population Growth.
725 Science (80-.). 289, 284–288. doi:10.1126/science.289.5477.284
726 Xu, B., Mao, D., Luo, Y., Xu, L., 2011. Sulfamethoxazole biodegradation and
727 biotransformation in the water-sediment system of a natural river.
728 Bioresour. Technol. 102, 7069–7076. doi:10.1016/j.biortech.2011.04.086
729 Xu, J., Wang, Z., Wei, X., Yang, S., Wang, J., Wang, S., 2013. The chlorination
730 process of crosslinked aromatic polyamide reverse osmosis membrane:
731 New insights from the study of self-made membrane. Desalination 313,
732 145–155. doi:10.1016/j.desal.2012.12.020
733 Zhao, F., Xu, K., Ren, H., Ding, L., Geng, J., Zhang, Y., 2015. Combined effects
734 of organic matter and calcium on biofouling of nanofiltration membranes. J.
735 Memb. Sci. 486, 177–188. doi:10.1016/j.memsci.2015.03.032
736 Zhou, C., Ontiveros-valencia, A., Nerenberg, R., Tang, Y., Zhou, C., 2019.

737 Hydrogenotrophic Microbial Reduction of Oxyanions With the Membrane
738 Biofilm Reactor 9, 1–14. doi:10.3389/fmicb.2018.03268

739
740
741
742
743
744
745
746
747
748
749
750
751
752

Type	Zeta potential (mV)	Contact angle (º)	Roughness	
			Ra (nm)	Rq (nm)
BWd[a]	-31.68 ± 4.89 ^{AB}	50.74 ± 2.96 ^{C}	32.01 ± 4.77 ^{B}	42.69 ± 5.26 ^{A}
BWt-NF	-35.19 ± 4.23 ^{A}	45.66 ± 1.55 ^{D}	32.18 ± 4.01 ^{B}	40.71 ± 5.04 ^{A}
BWt-UF	-22.49 ± 5.22 ^{B}	51.85 ± 2.14 ^{C}	4.77 ± 0.42 ^{C}	6.19 ± 0.47 ^{B}
SWd[a]	-30.53 ± 3.40 ^{AB}	29.48 ± 1.54 ^{E}	88.75 ± 28.89 ^{A}	98.71 ± 30.03 ^{A}
SWt-NF	-37.11 ± 4.42 ^{A}	68.19 ± 2.79 ^{A}	47.61 ± 12.05 ^{B}	58.64 ± 13.59 ^{A}
SWt-UF	-33.55 ± 4.48 ^{A}	60.23 ± 1.25 ^{B}	4.32 ± 0.63 ^{C}	5.74 ± 0.93 ^{B}

[a]Discarded RO membranes already reported (Morón-López et al., 2019).

Table 1. Zeta potential, contact angle and roughness of the transformed EoL membranes. Statistics analyses are shown per column, where each different capital letter indicates the significant differences between membranes at $p < 0.05$ after the one-way ANOVA.

Type	Air permeability (Barrer)	Air flux (J) ($Ncm^3 \cdot cm^{-2} \cdot s^{-1} \cdot cmHg^{-1}$)
BWd	$1.60 \cdot 10^{-7}$	$8.00 \cdot 10^{-3}$
BWt-NF	$1.01 \cdot 10^{-7}$	$5.06 \cdot 10^{-3}$
BWt-UF	$1.79 \cdot 10^{-4}$	$1.79 \cdot 10^{-2}$
SWd	$4.89 \cdot 10^{-9}$	$2.44 \cdot 10^{-4}$
SWt-NF	$4.81 \cdot 10^{-9}$	$3.01 \cdot 10^{-4}$
SWt-UF	$2.78 \cdot 10^{-5}$	$2.78 \cdot 10^{-3}$

* 1 Barrier = 10^{-10} $Ncm^3 \cdot cm \cdot cm^{-2} \cdot s^{-1} \cdot cmHg^{-1}$

Table 2. Air permeability and flux (J) at room temperature and pressure at 1 bar.

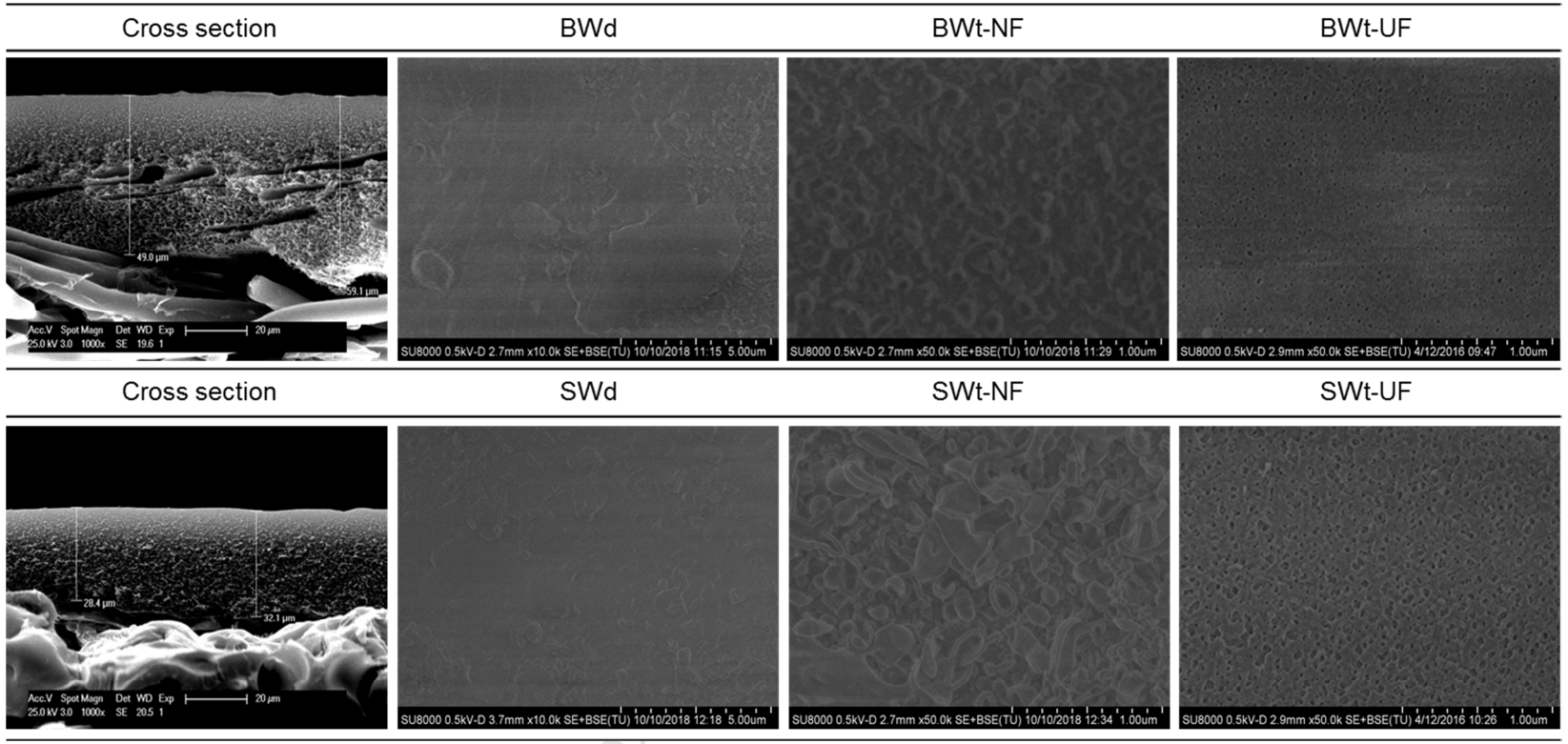

Fig.1. Cross-section and surface SEM images of the EoL desalination membranes before (BWd, SWd) and after chemical attack with NaOCl at doses of 6200 ppm·h (BWt-NF and SWt-NF) and 300000 ppm·h (BWt-UF and SWt-UF).

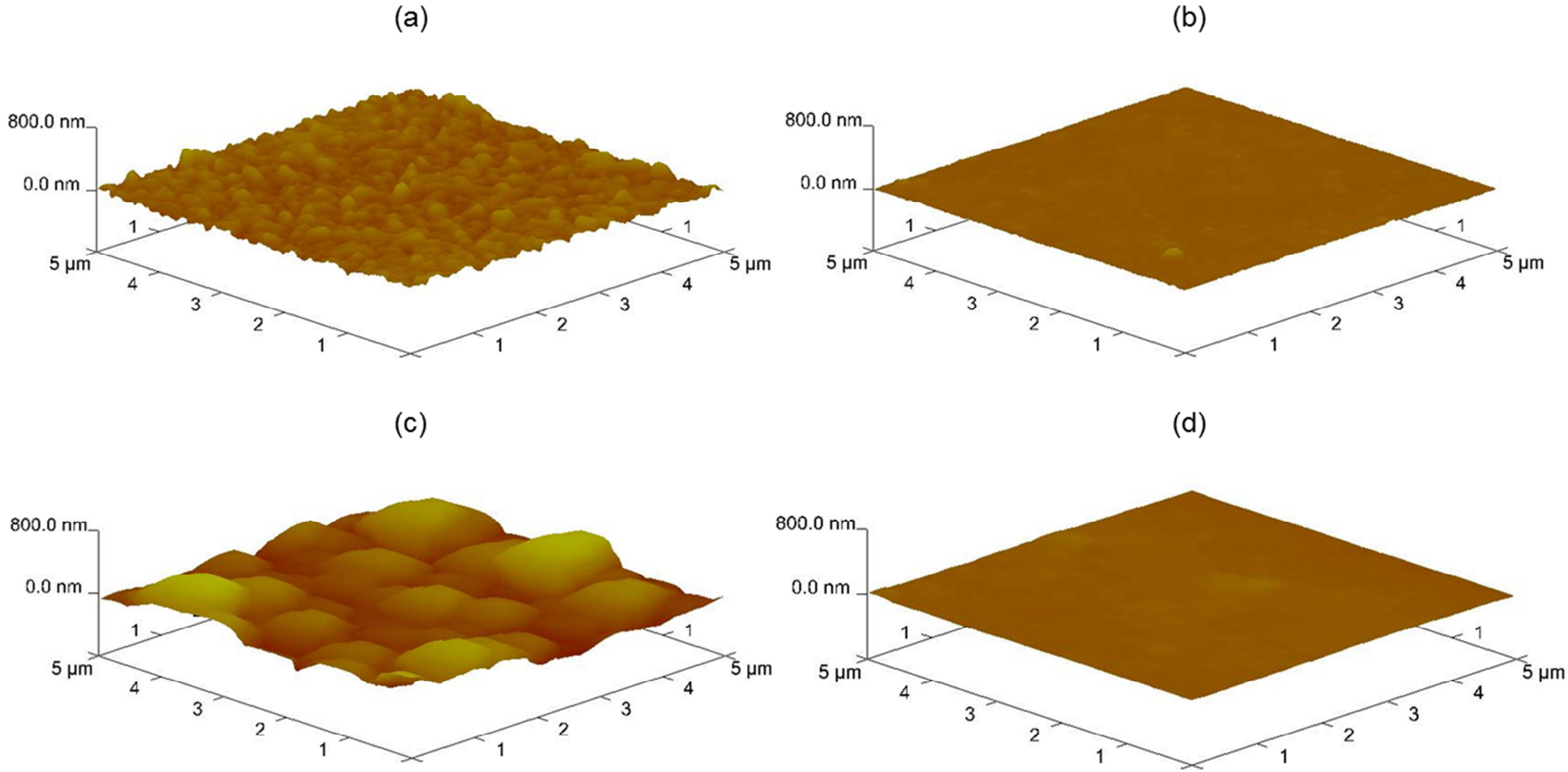

Fig.2. AFM images of membranes: (a) BWt-NF, (b) BWt-UF (c) SWt-NF and (d) SWt-UF

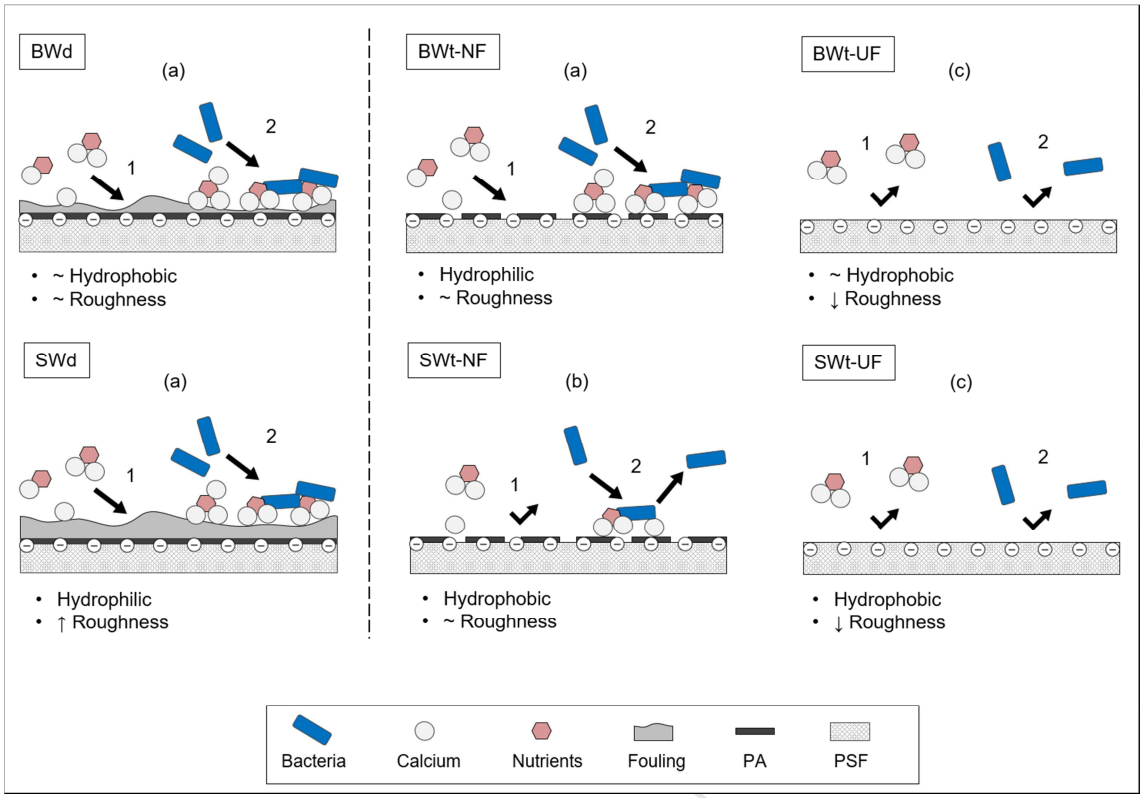

Fig. 3. Schematic illustration of early biofilm stages into tested EoL membranes. (1) Indicates the first conditioning stage, while (2) is bacterial deposition. Letters represent: (a) good conditioning and subsequent bacterial attachment; (b) bad conditioning and low bacterial deposition; (c) no conditioning and no bacterial attachment. The dotted line separates the untransformed discarded membranes from the transformed ones.

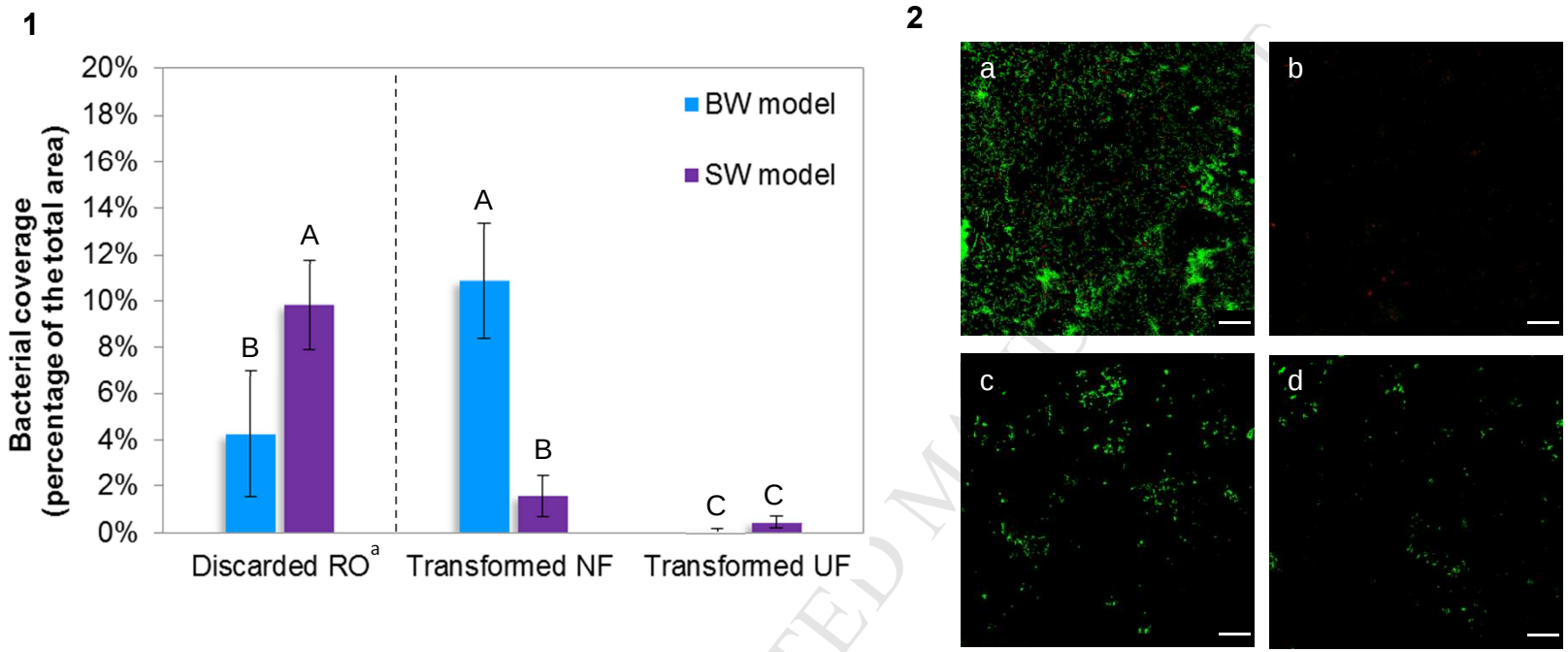

[a] These results have been already reported (Morón-López et al., 2019).

Fig. 4. Bacterial deposition on different transformed membrane surfaces: (**1**) Percentage of bacterial coverage. Statistic analyses shows different capital letters when indicating significant differences between membranes at $p < 0.05$ after a one-way ANOVA; (**2**) CLSM images after staining transformed membranes with the life/dead bacterial kit. (a) BWt-NF, (b) BWt-UF and (c) SWt-NF and (d) SWt-UF.

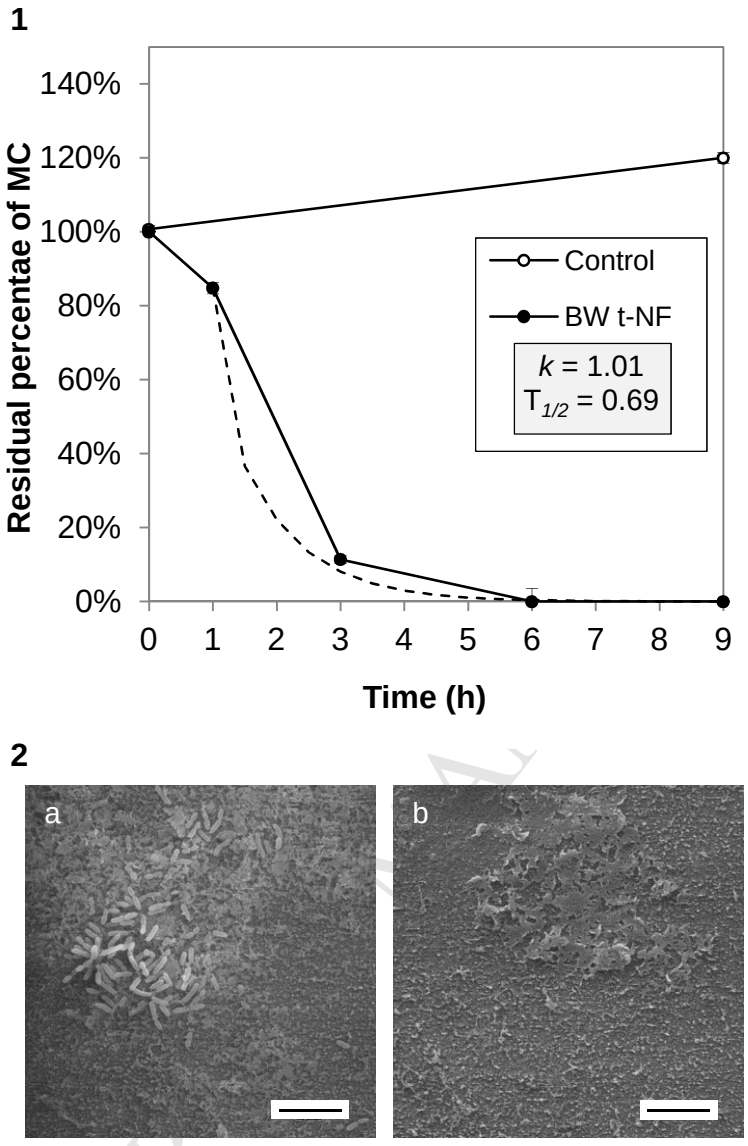

Fig. 5. MC degradation capability of strain IM-1 attached to the BWt-NF membrane. (**1**) MC degradation during the second MC exposure (after the acclimation time). The dotted line indicates the pseudo first-order model prediction. The MC error bars represent the standard deviation of two technical replicates. (**2**) The SEM images of the BWt-NF membrane surface with (**a**) strain IM-1 attached; (**b**) no bacterial deposition (control). Bar shows 5 μm.

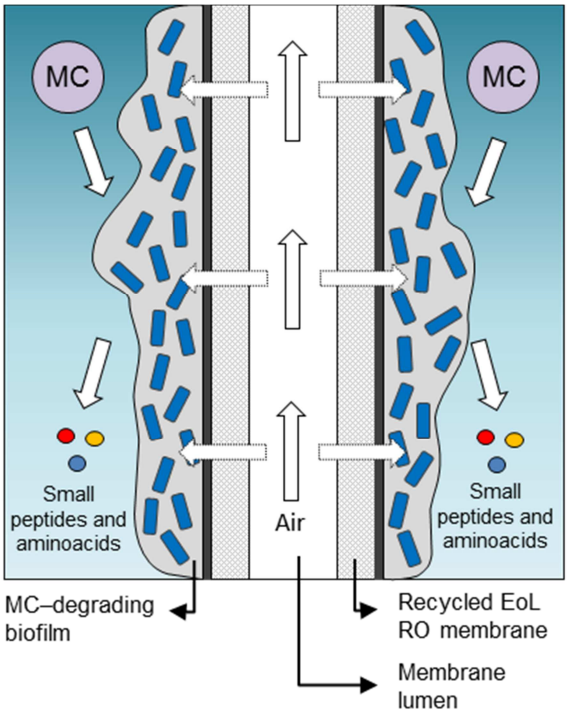

Fig.6. Schematic illustration of the aerobic MC-degrading biofilm attached onto recycled EoL RO membrane adapted to MBfRs.

Highlights

- Tested doses of chlorine trigger different changes on membrane surfaces depending on the polyamide nature and treated water sources during their lifespan (fouling).

- Chlorination process increase hydrophilicity and maintain roughness in some membranes, improving the surface conditioning and bacterial deposition.

- The chlorine attack does not affect the biological activity of the MC-degrading bacteria once attached into BWt-NF.

- Recycled thin film composite polyamide membranes allow competitive gas permeability at low pressure, which is a key characteristic for membrane biofilm reactors (MBfRs).